https://doi.org/10.5194/gmd-2021-244
Preprint. Discussion started: 21 July 2021

Geoscientific Model Development
Discussions

Modeling perennial bioenergy crops in the E3SM land model

Eva Sinha[1], Kate V. Calvin[2], Ben Bond-Lamberty[2], Beth A. Drewniak[3], Dan M. Ricciuto[4], Khachik Sargsyan[5], Yanyan Cheng[1,6], Carl Bernacchi[7,8], and Caitlin E Moore[8,9]

[1]Pacific Northwest National Laboratory, Richland, WA, United States
[2]Joint Global Change Research Institute, Pacific Northwest National Laboratory, College Park, MD, United States
[3]Argonne National Laboratory, Lemont, IL, United States
[4]Oak Ridge National Laboratory, Oak Ridge, TN, United States
[5]Sandia National Laboratories, Livermore, CA, United States
[6]Department of Industrial Systems Engineering and Management, National University of Singapore, Singapore
[7]Global Change and Photosynthesis Research Unit, USDA-ARS, Urbana, IL, United States
[8]University of Illinois at Urbana-Champaign, Urbana, IL, United States
[9]School of Agriculture and Environment, The University of Western Australia, Crawley, WA, Australia

Correspondence: Eva Sinha (eva.sinha@pnnl.gov)

Abstract. Perennial bioenergy crops are increasingly important for the production of ethanol and other renewable fuels, and as part of an agricultural system that alters the climate through its impact on biogeophysical and biogeochemical properties of the terrestrial ecosystem. The Energy Exascale Earth System Model (E3SM) Land Model (ELM) does not represent perennial bioenergy crops, however. In this study, we expand ELM's crop model to include perennial bioenergy crops whose production increases in modeled socioeconomic pathways owing to their potential for mitigating climate change. We focus on high-productivity miscanthus and switchgrass, estimating various parameters associated with their different growth stages and performing a global sensitivity analysis to identify and optimize these parameters. The sensitivity analysis identifies eight parameters associated with phenology, carbon/nitrogen allocation, and photosynthetic capacity as the most sensitive parameters for carbon and energy fluxes. We calibrated the model against observations collected at the University of Illinois Energy Farm for carbon and energy fluxes, and found that the model closely captures the observed seasonality and the magnitude of carbon fluxes. The model accurately represents the seasonality of energy fluxes, but their magnitude is not well captured. This work provides a foundation for future analyses of the interactions between perennial bioenergy crops and carbon, water, and energy dynamics in the larger earth system and can also be used for studying the impact of future biofuel expansion on climate and terrestrial systems.

https://doi.org/10.5194/gmd-2021-244
Preprint. Discussion started: 21 July 2021

Geoscientific Model Development
Discussions

1 Introduction

Agriculture occupies 11% of the global land (Klein Goldewijk et al., 2017; FAO, 2021) and can alter the regional and global climate through biogeochemical and biophysical impacts on the land surface (Seguin et al., 2007; Lombardozzi et al., 2020). Examples of biogeochemical impacts include large increase in CO_2 emissions resulting from the replacement of native vegetation with cropland (Seguin et al., 2007; Fargione et al., 2008). Although increased agricultural productivity results in enhanced CO_2 uptake during the growing season, different management practices can result in net increase in CO_2 and other greenhouse gas emissions such as methane and nitrous oxide (Verge et al., 2007; Searchinger et al., 2008). The biophysical impacts on the land surface include modification of the surface energy and water budget. For example, agricultural intensification and the resulting increase in evapotranspiration causes a decrease in extreme summer temperature and an increase in precipitation (Mueller et al., 2016) while the use of cover crops impacts regional temperature and causes warmer winters (Lombardozzi et al., 2018).

Earth System Models (ESMs) that are used for climate projections should have adequate representation of crops due to the impact of agriculture on regional and global climate. However, most ESMs represent crops as generic-grass that fails to capture the various phenological phases of crops and differences across various crop species (Levis, 2010; McDermid et al., 2017; Moore et al., 2021). This simplistic representation of crops underestimates gross primary productivity and latent heat flux from agricultural-dominated regions (Lombardozzi et al., 2020). To address this shortcoming and to improve the simulation of carbon and water fluxes, several land model components of ESMs are now simulating major crops. For example species specific crops are now represented in the Community Land Model (Levis et al., 2012; Drewniak et al., 2013), E3SM Land Model (Burrows et al., 2020), Joint UK Land Environment Simulator (Osborne et al., 2015), Noah-MP-Crop (Liu et al., 2016), ORCHIDEE (Wu et al., 2016), and Simple Biosphere Model (Lokupitiya et al., 2009).

Perennial bioenergy crops are not well represented in ESMs, despite large increases in bioenergy production projected in modeled socioeconomic pathways for meeting future energy demands and for mitigating climate change. Energy crops are expected to account for a significant portion of bioenergy in the U.S. by 2040 (Langholtz et al., 2016). The quantity of bioenergy production required in the future is highly uncertain and will depend on the future energy demand and radiative forcing level, among other factors. For example, it is estimated that to limit future warming to 1.5°C, 40 – 310 EJ yr^{-1} of bioenergy will be required (IPCC, 2018). Another study estimates future land area required for bioenergy production to range between 120 – 470 million ha for the RCP4.5 mitigation scenario and between 250 – 1500 million ha for the RCP2.6 mitigation scenario (Popp et al., 2017). To understand the impact of such increased biomass production on carbon, water, and energy fluxes, perennial bioenergy crops should be adequately represented in ESMs. This has been achieved in select land components of ESMs. For example, Song et al. (2015) incorporated *Miscanthus* × *giganteus* (miscanthus) and two different varieties of switchgrass in ISAM model and used it to study the spatial and temporal patterns in biomass yield in the eastern United States. Zhu et al. (2017) parameterized and validated Community Land Model (CLM) version 4.5 for miscanthus and switchgrass and estimated carbon and surface energy balance from the growth of these crops across the Continental United States. Li et al.

https://doi.org/10.5194/gmd-2021-244
Preprint. Discussion started: 21 July 2021

Geoscientific Model Development Discussions

(2018) implemented four major perennial bioenergy crops in the global dynamic vegetation model, ORCHIDEE, and utilized it to compare simulated vs. observed biomass yield. Cheng et al. (2020) incorporated two perennial bioenergy crops into CLM version 5 and found that compared to traditional bioenergy crops, perennial crops have higher carbon uptake and lower nutrient requirement that increases their suitability for future bioenergy production. Littleton et al. (2020) modified JULES land surface model to simulate the growth and harvest of perennial bioenergy crops and applied the updated model for estimating global annual yield of miscanthus under the future climate. Adequate representation of perennial bioenergy crops requires optimizing the various crop parameters and quantifying the parametric uncertainty.

Calibrating ESMs crop parameters poses significant challenge due to the large number of parameters and considerable computational cost of calibration. ESMs simulate various terrestrial and biogeochemical processes by utilizing a vast array of parameters that can contribute large uncertainties in model predictions (Lambert et al., 2013; Qian et al., 2018). The ESM crop-models often use default global parameter values rather than crop- and region-specific values that results in large biases between model simulated and observed fluxes (Cheng et al., 2021). These biases can be reduced by calibrating the model and finding the optimal parameter ranges (Lu et al., 2018). Model calibration is often preceded by sensitivity analysis for identifying the most influential parameters for various model outputs (Ricciuto et al., 2018). However, model complexity and long simulation time required for achieving biogeochemical equilibrium makes sensitivity analysis and calibration computationally expensive. These challenges have caused several studies to either modify the crop parameters based on values in literature or field observations (Zhu et al., 2017; Li et al., 2018; Boas et al., 2021), or to calibrate the model by utilizing one-at-time (OAT) approach that varies a single model parameter at a time (Song et al., 2013, 2015; Cheng et al., 2020; Littleton et al., 2020). However, both these approaches fail to account for the impact of joint parameter variability on model outputs (Ricciuto et al., 2018; Qian et al., 2018). To overcome these challenges, studies are now constructing ESM surrogates followed up by global sensitivity analysis (GSA) and model calibration using these surrogates (Lu et al., 2018; Ricciuto et al., 2018; Lu and Ricciuto, 2019).

The objective of this study is to expand the crop model in the Energy Exascale Earth System Model (E3SM) land component (ELM) to include two perennial bioenergy crops - miscanthus (*Miscanthus* $\times$ *giganteus*) and switchgrass (*Panicum virgatum* L.). The model is calibrated to simulate carbon and energy fluxes by developing ELM surrogates, conducting a GSA, and performing Bayesian calibration using observational data. Miscanthus and switchgrass are perennial grasses with phenological stages distinct from annual crops. Therefore, in this study we expand the ELM crop model to include perennial grasses and parameterize the updated model for miscanthus and switchgrass.

2 Model Development

The E3SM land model version 1 (ELMv1) is branched from CLM version 4.5 (CLM4.5) (Oleson et al., 2013). The differences between ELMv1 and CLM4.5 are described in Burrows et al. (2020) and Ricciuto et al. (2018). For capturing the impact of agriculture on climate and vice-versa, ELM includes representation of annual crops, maize, soybean, and spring wheat in its

https://doi.org/10.5194/gmd-2021-244
Preprint. Discussion started: 21 July 2021

crop model (Levis et al., 2012; Drewniak et al., 2013). Recent updates to the crop model include the implementation of dynamic root modeling (Drewniak, 2019) and climate driven planting date estimation. The crop models in both CLM4.5 and ELMv1 do not include representation of perennial crops. Perennial crops are distinctly different from annual crops. For example, differences in albedo and rooting depth result in increased evapotranspiration in perennial crops that can have a cooling effect (Georgescu et al., 2011). Additionally, perennial crops such as miscanthus and switchgrass require fewer fertilizer inputs and reduce nitrogen leaching compared with maize and soybean (Smith et al., 2013). This study implements perennial crop modeling in ELM and the subsections below describe the phenology, carbon and nitrogen allocation, and harvest for perennial crops.

2.1 Phenology

The perennial crop phenology consisted of three distinct phases: crop emergence, leaf onset, and leaf senescence. The perennial crops are planted once and the crops re-grow from underground lingotubers each year. In ELM the crop plantation in the first year and re-emergence in the following years occurs between the minimum and maximum plant emergence date when the temperature thresholds are met (Eq. 1 – 3).

$$T_{10d} < \overline{T}_p \tag{1}$$

$$T_{10d}^{min} < \overline{T}_p^{min} \tag{2}$$

$$\overline{d}_{plant}^{min} \leq jday \leq \overline{d}_{plant}^{max} \tag{3}$$

where T_{10d} is the 10-day running mean of T_{2m} (the simulated 2-m air temperature during each model time step) and T_{10d}^{min} is the 10-day running mean of T_{2m}^{min} (the daily minimum of T_{2m}). $\overline{T}_p$ and $\overline{T}_p^{min}$ are crop-specific coldest plant emergence temperatures. $\overline{d}_{plant}^{min}$ and $\overline{d}_{plant}^{max}$ are the crop-specific minimum and maximum plant emergence date, respectively, and jday is the julian day. All variables with an accent bar are model parameters and ones without an accent bar are model estimated values. The $\overline{T}_p^{min}$ parameter was set to 273.15K and $\overline{d}_{plant}^{min}$ and $\overline{d}_{plant}^{max}$ parameters were set to March 1^{st} and May 1^{st}, respectively for both miscanthus and switchgrass.

The leaf onset starts when the growing degree days (GDD) accumulated (Eq. 4) since plant emergence exceeds the crop-specific minimum GDD requirement (Eq. 5).

$$GDD^n = GDD^{n-1} + (T_{s,3} - T_{frz}) \times f_{day} \tag{4}$$

$$GDD^n = \overline{GDD}^{min} \tag{5}$$

where GDD^n is the GDD accumulated at time step n (°day), $T_{s,3}$ is the temperature of the third soil layer (K), T_{frz} is the freezing point of water (273.15 K), f_{day} is the model time step (day), $\overline{GDD}^{min}$ is the minimum GDD requirement (°day).

https://doi.org/10.5194/gmd-2021-244
Preprint. Discussion started: 21 July 2021

The leaf senescence occurs when the temperature and leaf age criteria are met (Eq. 6 – 7).

$$T_{10d} < \overline{T}_s \tag{6}$$

$$n_{days\ on} > \overline{n}_{min} \tag{7}$$

where $\overline{T}_s$ is the crop-specific senescence temperature, $n_{days\ on}$ is the leaf age in days, and $\overline{n}_{min}$ is the crop-specific minimum leaf age.

2.2 C and N Allocation

Similar to the annual crops being modeled in ELM, carbon and nitrogen assimilation in the perennial crops is based on phenological stages. The carbon/nitrogen (CN) allocation is simulated throughout the growing period; starting in the leaves, stem, and fine roots with leaf emergence, and ending at the time of the harvest. The CN ratios in the leaf, stem, and roots vary all through the growth period and are modeled based on CLM4.5 carbon and nitrogen allocation scheme (Oleson et al., 2013). Time varying allocation coefficients are used for estimating the fraction of carbon that is assigned to the leaf, steam, and fine roots (Eq. 8 – 10). These coefficients are similar to the allocation coefficients used for annual crop phase between leaf emergence and grain fill. The stem and fine root coefficients are the same as the annual crop coefficients while the leaf coefficient has $\overline{GDD}_{mat}$ (growing degree days required for maturity) replacing the heat unit index of the annual crops.

$$a_{froot} = \overline{a}^i_{froot} - (\overline{a}^i_{froot} - \overline{a}^f_{froot})\frac{GDD_{T2m}}{\overline{GDD}_{mat}} \tag{8}$$

$$a_{leaf} = (1 - a_{froot})\frac{\overline{a}^i_{leaf}\left(e^{-\overline{b}} - e^{-\overline{b}\frac{GDD_{T2m}}{\overline{GDD}_{mat}}}\right)}{e^{-\overline{b}} - 1} \tag{9}$$

$$a_{livestem} = 1 - a_{froot} - a_{leaf} \tag{10}$$

where, $\overline{a}^i_{froot}$, $\overline{a}^f_{froot}$, and $\overline{a}^i_{leaf}$ are initial and final values of root and leaf carbon allocation coefficients. $\overline{b}$ is an exponential factor used in leaf carbon allocation, $\overline{GDD}_{mat}$ is the GDD required for the crop to reach maturity, and GDD_{T2m} is the GDD for 2m air temperature.

2.3 Harvest

The perennial crop harvest occurs in a single time step after occurrence of the leaf senescence. During harvest, C and N stored in above-ground biomass comprised of leaf and live stem are removed. 70% of the available C and N contributes to food/biofuel production and the remainder is transferred to the litter pool (Zhu et al., 2017; Cheng et al., 2020).

3 Model Evaluation

In order to identify the impact of model parameters on output QoIs, as well as to quantify and reduce predictive variance associated with these uncertain parameters, we will first construct a surrogate approximation of the model across a range of variability of the parameters, followed by global sensitivity analysis, and Bayesian calibration of this pre-constructed surrogate.

3.1 Model Simulation and Surrogate Construction

A total of twenty perennial crop parameters related to crop phenology, CN allocation, and photosynthetic capacity were selected for the surrogate construction, global sensitivity analysis and model calibration (Table 1). We identified the input range for these parameters through literature review. If an input range for a parameter was not available in the literature then it was set based on expert judgement. The twenty parameters were randomly varied within their input range for 2000 ELM simulations. We used the Offline Land Model Testbed for 2000 ensemble ELM runs, each of which ran for 200 years in the accelerated spin-up mode and 200 years in the nonaccelerated spin-up mode, followed by a transient run from 1850 to 2008. For the transient run Global Soil Wetness Project Phase 3 (GSWP3) data was used for the meteorological forcing. The model output was postprocessed by estimating daily average over the last ten years of the transient run for the four output quantities of interest (QoIs) — gross primary productivity (GPP), ecosystem respiration (ER), latent heat flux (LE), and sensible heat flux (H). The estimated daily average for all ensemble members was then used as training inputs for developing surrogates. We employed Polynomial chaos (PC) surrogate form for developing surrogates as it provides flexible representation of the inputs and outputs as random variables (Ghanem and Spanos, 1991), and, at the same time, allows for exact analytical extraction of global sensitivity indices via variance decomposition (Crestaux et al., 2009). In our case, where the inputs are randomly and uniformly sampled over their respective ranges, the surrogate construction reduces to a polynomial regression (Sargsyan, 2017). Finally, due to large number of input parameters, we employed Bayesian compressive sensing algorithm (Sargsyan et al., 2014; Ricciuto et al., 2018) to regularize the regression, arriving at a sparse polynomial set with only the relevant PC bases activated. The surrogate construction, the associated global sensitivity analysis as well as the surrogate-enabled model calibration are carried out using the UQ Toolkit (Debusschere et al., 2016).

3.2 Global Sensitivity Analysis

Sobol sensitivity indices were used to examine the impact of parametric uncertainty on model outputs (Saltelli et al., 2010; Sobol, 2001). These indices provide an estimate of the fraction of variance contributed by each parameter or group of parameters towards the total variance in the output variable (Ricciuto et al., 2018). A major convenience of using PC surrogates is that one can extract the sensitivity indices with analytically available formulae without any additional sampling (Crestaux et al., 2009). In this study, we evaluate the main effect sensitivity that examines the contribution of one parameter at a time on the total variance (Figure 2).

3.3 Site Data

The observational data utilized for model calibration was collected at the University of Illinois Urbana-Champaign (UIUC) Energy Farm located in the Midwest region of the United States. The mean annual precipitation at the UIUC Energy Farm is 1009 mm and the mean annual temperature is 10.9°C with large seasonal variation ranging from monthly minimum below -5°C in winter to monthly maximum above 25°C in summer (Moore et al., 2021). The soil at the UIUC Energy Farm is deep and poorly drained silty clay loam. Both miscanthus and switchgrass plots were planted in the spring of 2008, however

https://doi.org/10.5194/gmd-2021-244
Preprint. Discussion started: 21 July 2021

supplementary miscanthus was planted in 2009 and 2010 due to to poor establishment in 2008 (Anderson-Teixeira et al., 2013). Nitrogen fertilizer was applied every year to switchgrass and from 2014 – 2018 to miscanthus at the rate of 56 $kg\ ha^{-1}$. Switchgrass was harvested at the end of the growing season in November or December, while miscanthus was harvested in the winter months of February or March. Eddy covariance flux towers at the center of the plots measure carbon, water, and energy fluxes at 30-min intervals, along with common meteorological variables (Zeri et al., 2011; Moore et al., 2020). Gross primary productivity (GPP) and ecosystem respiration (ER) were calculated from flux tower net ecosystem exchange values as per Moore et al. (2020). The flux tower derived GPP and ER are referred to as observed GPP and ER, respectively, in the remainder of the manuscript. GPP, ER, LE, and H values from 2008 – 2019 for miscanthus and from 2008 – 2016 for switchgrass were used for calibrating the ELM-Crop model.

3.4 Bayesian calibration via Markov chain Monte Carlo

Bayesian inference was utilized for calibrating model parameters to improve the model performance with respect to site data (Tarantola, 2005). Specifically, we employ Markov chain Monte Carlo (MCMC) which samples input parameter space with an acceptance/rejection mechanism relying on the match of the model with the observational data encapsulated by a likelihood function. However, MCMC typically requires infeasibly large number of model evaluations before it arrives to a representative set of parameter samples. For this reason, we employ the pre-constructed, computationally inexpensive surrogate models in the MCMC loop. For each QoI, a calibration window was first identified for both perennial bioenergy crops since all four QoIs had low or negligible values during the non-growth period. We tested four different calibration windows for GPP that excluded the winter months with minimal crop growth (Table A1). We found that a calibration window of 60 – 330 for miscanthus and 60 – 270 for switchgrass resulted in both low RMSE and percent bias between observations and mean of the posterior simulations. For both miscanthus and switchgrass, the same calibration window was used for all four QoIs.

https://doi.org/10.5194/gmd-2021-244
Preprint. Discussion started: 21 July 2021

Table 1. Descriptions, input ranges, and sources of information used for the eighteen input parameters varied in this study.

Parameter	ELM variable	Units	Description	Minimum	Maximum	Source
$\overline{T}_p$	planting_temp	K	Average 10-day temperature required for plant emergence	275	285	1
$\overline{GDD}^{min}$	gddmin	°day	Minimum growing degree days	50	320	2
$\overline{T}_s$	senescence_temp	K	Average 10-day temperature for leaf senescence	280	290	1
$\overline{n}_{min}$	min_days_senes	days	Minimum leaf age to allow for leaf senescence	90	120	3
$\overline{a}^i_{froot}$	arooti	-	Root CN allocation coefficient	0.05	0.3	4
$\overline{a}^f_{froot}$	arootf	-	Root CN allocation coefficient	0.05	0.2	4
$\overline{a}^i_{leaf}$	fleafi	-	Leaf CN allocation coefficient	0.5	0.95	4
$\overline{b}$	bfact	-	Exponential factor for leaf CN allocation	0.05	0.15	2
$\overline{GDD}_{mat}$	hybgdd	°day	Growing degree days required for maturity	1600	2000	2
	leafcn	$gC\ gN^{-1}$	Leaf CN ratio	15	35	2
	livewdcn	$gC\ gN^{-1}$	Live wood CN ratio	40	60	2
	frootcn	$gC\ gN^{-1}$	Fine root CN ratio	20	50	5
	graincn	$gC\ gN^{-1}$	Grain CN ratio	25	60	6
	laimx	-	Maximum leaf area index used in CNVegStructUpdate	5	12	4
	slatop	$m^2\ gC^{-1}$	Specific leaf area (SLA) at top of canopy, projected area basis	0.01	0.07	4
	i_vc	$umol\ CO_2\ m^{-2}\ s^{-1}$	Intercept of the relationship between leaf N per unit area and vcmax	3	35	4
	s_vc	$umol\ CO_2\ m^{-2}\ s^{-1}$	Slope of the relationship between leaf N per unit area and vcmax	6	70	4
	br_mr	$umol\ CO_2\ m^{-2}\ s^{-1}$	Base rate for maintenance respiration (MR)	1.26E-06	3.75E-06	7
	q10_mr	-	Temperature sensitivity for MR	1.3	3.3	7
	mbbopt	-	Ball–Berry model equation slope	4	12	8

Note: The ranges are based on 1) observations 2) expert judgement (in the case where there is insufficient literature, but within 50% would be inappropriate) 3) Li et al. (2018) 4) Cheng et al. (2020) 5) Dietzel et al. (2017) 6) Ma and Dwyer (2001) 7) Ricciuto et al. (2018) 8) Personal communication with Dr. Dan Ricciuto

https://doi.org/10.5194/gmd-2021-244
Preprint. Discussion started: 21 July 2021

4 Results

4.1 Ensemble Evaluation

The ensemble captures observed seasonality and peak GPP values for both perennial bioenergy crops (Figure 1 A and B). The seasonality of the perennial bioenergy crops, marked by the start and end of the growing season, is around 50 days longer than that of traditional maize grown in the midwestern USA (Cheng et al., 2020). The modified ELM model captures this longer growing season. Leaf onset for both perennial bioenergy cropping systems starts at approximately the same time but switchgrass GPP increases and declines earlier than miscanthus. The resulting slightly shifted growing seasons for the two perennial bioenergy crops was well captured by the ELM ensemble runs. Similar to seasonality, the model closely captures GPP values during the peak growing season, including the large observed interannual variability (light red lines in Figure 1 A and B).

The model simulates ecosystem respiration well for both crops, during both growth and non-growth periods (Figure 1 C and D). During the growing season, the ensemble captures the full range of ER values. However, during the non-growth period the low observed ER values were simulated only by a small fraction of the ensemble members with the majority of ensemble members over predicting the ER during this period. The model simulated large negative spikes in late fall, is a caveat of the crop model eliminating excess maintenance respiration pool at harvest time (Oleson et al., 2013). This excess maintenance respiration pool is maintained by the model to supply carbon to plants during periods of low photosynthesis but is not required after harvest.

The ensemble captures the seasonality and observed extent of the energy fluxes during the growth phase (Figure 1 E – H). Similar to ER, the full range of both LE and H during the growing season are captured by the ensemble. However, during the non-growth period the model ensemble underestimates both the observed mean and interannual variability in LE. For H, the ensemble simulation is close to the observed mean during the non-growth period but does not capture the large interannual variability during this period.

4.2 ELM Surrogate Performance

The ELM surrogates provided fairly accurate representation of ELM simulations. We utilized 1600 of the 2000 ELM simulations for developing the surrogates using PC surrogate form and 400 simulations for testing the accuracy of the surrogates. The training data points were close to center diagonal line, representing agreement between surrogate and ELM simulations (green dots in Figure A1 and A2). The daily root mean squared error (RMSE) and relative RMSE between surrogate and ELM simulations for testing data points was relatively low during the growing season for all four QoIs for both perennial bioenergy crops, with few outliers during the non-growth period (Figure A3 and A4). These outliers during non-growth season however, did not impact the results of calibration as they fell outside of the calibration window and were therefore not utilized for GSA and calibration (Section 3.4). The average daily RMSE for miscanthus was 0.67 ($gC\ m^{-2}\ day^{-1}$) for GPP, 0.5 ($gC\ m^{-2}\ day^{-1}$)

Geoscientific Model Development Discussions

for ER, 2.92 ($W\ m^{-2}$) for LE, and 2.21 ($W\ m^{-2}$) for H while the relative RMSE for the same QoIs was 0.16, 0.12, 0.32, and 0.2, respectively. For switchgrass the average daily RMSE was 0.63 for GPP, 0.52 for ER, 2.82 for LE, and 2.32 for H while the relative RMSE for the same QoIs was 0.34, 0.13, 0.31, and 0.36, respectively.

4.3 Parameter Sensitivity

The most sensitive parameters for GPP, LE, and H vary with phenological state (Figure 2 A, B, and E – H) while for ER they remain the same throughout the year, although their relative sensitivity changes with phenological stage (Figure 2 C and D). For both perennial bioenergy crops, the parameter associated with stomatal conductance (`mbbopt`) and specific leaf area (`slatop`) were the most sensitive parameters for all four QoIs while parameter associated with leaf CN allocation (`leafcn`) was influential for GPP and ER. These parameters were most influential for GPP only during the growth phase but for ER, LE, and H they remain sensitive for most of the year. The parameter controlling leaf senescence (`senescence_temp`) was one of the most influential parameters during the leaf senescence period for all four QoIs. During the non-growth period, the temperature sensitivity for maintenance respiration (`q10_mr`) parameter was the most sensitive parameter for ER. For GPP, LE, and H, during the leaf emergence phase, the parameters controlling leaf onset (`gddmin` and `planting_temp`) exhibit high sensitivities.

4.4 Model Calibration

The optimized parameter values for select parameters were similar across the four QoIs (Table 2). These values represent the maximum a posteriori (MAP) estimates of the optimized parameter range obtained after conducting GSA for the five most sensitive parameters (Figure A5 – A8). Since all four QoIs for miscanthus and switchgrass were calibrated separately, sightly different optimized parameter values were predicted for the different QoIs. For miscanthus, the optimal range of `planting_temp`, `gddmin`, `senescence_temp`, and `mbbopt` and for switchgrass the optimal range of `planting_temp`, `gddmin`, and `leafcn` are relatively close across the four QoIs. A reliable range for optimal `senescence_temp` for switchgrass is not obtained since `senescence_temp` is only sensitive during the last few months of the year that fall outside the calibration window for switchgrass. Additionally, the optimized value of `leafcn` for miscanthus GPP, `mbbopt` for miscanthus LE, `slatop` for switchgrass GPP and ER, and `mbbopt` for switchgrass ER are less reliable as the probability density function (pdf) of the optimized parameter are skewed towards either side of the input range (Figure A5, A7), indicating a degree of overfitting or a need to increase the parameter range. The optimized value of `slatop` for both perennial bioenergy crops and the optimized value of `mbbopt` for switchgrass are spread across most of the input range, signifying potential over-calibration given that the QoIs are extremely sensitive to `slatop` and `mbbopt` parameters.

The calibrated GPP closely matches the observations for the timing of leaf onset, timing of peak GPP, the sharp increase before peak GPP, the peak GPP, and the timing of leaf senescence for both perennial bioenergy crops (Figure 3 A and B black line and green shading). Overall, the posterior GPP estimates explained more than 90% of the observed daily variance within the calibration window and for all year round for both miscanthus and switchgrass (Table 3). The percent bias for miscanthus was less than 2% and for switchgrass was less than 7%. During late fall, the posterior estimate of switchgrass GPP have a large spread due to the optimal range for switchgrass `senescence_temp` not being identified that in turn spreads leaf senescence over the entire input range in the posterior ensemble.

The calibrated ER closely matches the observations during the growing period and is slightly higher than the observations during the non-growing season for both crops (Figure 3 B and D). Similar to GPP, the posterior ER estimates explained close to 90% of the observed daily variance. The higher observed percent bias during the calibration window for both perennial bioenergy crops, despite closely matching the observations, can most likely be attributed to the daily variations.

The posterior estimates of both energy fluxes capture the seasonality in the observations, although a larger fraction of daily variation is explained by the latent heat flux (80%) than by the sensible heat flux (10 – 40%) (Table 3). The higher explanatory power of LE for observed daily variation is likely due to increased amount of moisture available during summer for evapotranspiration that results in LE dominating the energy balance. Similar to ER, the large percent bias for LE despite closely matching the observations is likely due to difference in values at a daily timescale. Although, the posterior H estimates capture the seasonality in the observations they fail to capture the observed magnitude during the growing season, especially for switchgrass. It is also noteworthy that the observed daily average used for calibration has a higher signal to noise ratio for both the energy fluxes than for the carbon fluxes, likely contributing to lower calibration accuracy for the energy fluxes.

5 Discussion

Only a handful of parameters dominate the sensitivity of carbon and energy fluxes for the two perennial bioenergy crops. The ELM crop model utilizes a large number of parameters each with its own uncertainty that results in a large spread in the simulated fluxes. The sensitivity analysis performed in this study shows that eight out of more than 100 parameters used for the ELM crop model, dictate the uncertainty in modeled carbon and energy fluxes. This finding can assist in streamlining future model calibration efforts. Similar findings were also made for ELM simulated carbon cycle outputs from multiple plant functional types (Ricciuto et al., 2018). We find that for both carbon and energy fluxes parameters controlling the timing of leaf senescence (`senescence_temp`), onset of leaves (`gddmin`), photosynthetic capacity (`slatop`), and stomatal conductance (`mbbopt`) are among the most sensitive parameters. Additionally, for GPP and ER the parameter controlling leaf CN allocation (`leafcn`), for ER the parameter controlling maintenance respiration (`q10_mr`), and for LE and H the parameter controlling plant emergence (`plantemp`) were also highly sensitive.

Some of the most influential parameters identified in this study had been previously identified while others had not been previously recognized. Another study modeling miscanthus and switchgrass using CLM5, also identified `slatop` and `fleafi` as sensitive parameters for GPP, ER, and LE (Cheng et al., 2020) . However, Cheng et al. (2020) also identified parameters associated with photosynthetic capacity (`s_vc` and `i_vc`) as sensitive parameters. These two parameters were considered in our analysis but were not found to be sensitive for carbon or energy fluxes. The parameters associated with phenology (`gddmin`,

https://doi.org/10.5194/gmd-2021-244
Preprint. Discussion started: 21 July 2021

Geoscientific Model Development Discussions

plantemp, senescence_temp), stomatal conductance (mbbopt), and maintenance respiration (q10_mr) had not been identified before as influential for modeling carbon and energy fluxes for perennial crops. These difference are likely due to one or more of three major differences in these two studies. First, ELM and CLM5 both have several differences between them despite branching from the same model (CLM4.5). For instance, ELM now incorporates dynamic root modeling (Drewniak, 2019), climate driven planting date estimation, and perennial crop modeling while CLM5 includes the implementation of Fixation and Uptake of Nitrogen (FUN) and Leaf Use of Nitrogen for Assimilation (LUNA). The FUN model accounts for the carbon cost of nitrogen acquisition (Shi et al., 2016) while the LUNA model accounts for leaf nitrogen utilization in its photosynthetic capacity estimation (Ali et al., 2016). Second, both miscanthus and switchgrass are modeled as annual crops by Cheng et al. (2020) while in this study they are modeled as perennial crops to accurately capture various phenological stages, including crop emergence, leaf onset, growing season length, and leaf senescence, of the two crops that are quite distinct from annual crops. Third, Cheng et al. (2020) conducted sensitivity analysis by varying ten samples at equal increments within the input range, one parameter at a time. This approach ignores the effect of parameter interactions. The GSA approach utilized in this study accounts for parameter interactions by randomly varying all parameters within their input range to generate 2000 parameter samples for running ELM. Additionally, ELM surrogates were developed from the outputs of 2000 ELM runs that were then employed for surrogate based GSA. Due to these differences across the two studies, the optimized parameter values obtained in this study were compared to the literature rather than among themselves.

The optimized parameter range for slatop is similar in magnitude to observations collected at various sites. A study comparing photosynthetic rate among fourteen miscanthus genotypes observed slatop to range between 0.021 – 0.031 ($m^2\ g^{-1}$) (Jiao et al., 2016). Observational estimates for switchgrass slatop have varied between 0.014 – 0.023 (Trócsányi et al., 2009; Tian et al., 2015). A study comparing leaf photosynthetic rates among the two perennial bioenergy crops found slatop for miscanthus to be higher (0.015) than slatop for switchgrass (0.012) (Dohleman et al., 2009). The calibrated value estimated for slatop in this study ranges from 0.02 – 0.07 ($m^2\ gC^{-1}$) (Table 2) that is equivalent to 0.01 – 0.03 ($m^2\ g^{-1}$) (assuming the leaf carbon content is 45% of leaf weight) and falls within the observed range. Slatop has been observed to vary with the growing season and with light availability. Variation with the growing season resulted in peak value being observed earlier in the season followed by a gradual decline (Dohleman et al., 2009; Tian et al., 2015) while variation with light resulted in higher observed slatop for shaded canopy at the bottom of the plant and lower slatop at the top of the canopy (Trócsányi et al., 2009). Currently parameters in ELM-crop do not vary with the growing season or light availability.

Similar to slatop, the calibrated value of q10_mr is comparable to observations. Studies examining the impact of temperature sensitivity on soil respiration found q10_mr to range between 1.6 – 3.2 with an average of 3.0 for miscanthus (Yazaki et al., 2004; Robertson et al., 2017) and to range between 2.3 – 3.8 with an average of 2.7 for switchgrass (Lee et al., 2007; Skinner and Adler, 2010). Variability across the year was also observed in q10_mr with highest values being observed during the growth period and lowest values during winter months (Robertson et al., 2017). The q10_mr range estimated in this study (Table 2) is close to observations but stays constant throughout the year in ELM. Interestingly, a study calibrating CLM4.5 for coniferous forest found that q10_mr of 2.5 better captured the observed seasonality of ER for needleleaf evergreen temperate forest (Duarte et al., 2017).

6 Conclusions

This study implements perennial crop modeling in ELM and parameterizes the model for miscanthus and switchgrass using observational data on carbon and energy fluxes from the midwest United States. All four QoIs capture the observed seasonality and simulated carbon fluxes (GPP and ER) closely match the observations, however, the magnitude of energy fluxes (LE and H) was not well captured and warrants further exploration in future studies. The poor simulation of energy fluxes could be either due to lack of accurate process representation or due to relevant parameters not being considered for calibration or large signal to noise ratio in the observations. Future studies can explore calibrating model outputs related to water budgets along with calibrating the model using spatially varying site data.

Our modeling study lays the groundwork for future studies that examine the impact of perennial bioenergy crop expansion and provides valuable insights for improving representation of other crops in ESMs. Future research can utilize the parameterized perennial bioenergy crop model developed in this study to examine the impact of future perennial bioenergy expansion on carbon, water, and energy budgets. Additionally, future crop modeling studies that perform global sensitivity analysis can utilize only the most sensitive parameters identified in this study to reduce the surrogate models dimensionality and for improving the accuracy of the surrogate models.

https://doi.org/10.5194/gmd-2021-244
Preprint. Discussion started: 21 July 2021

Geoscientific Model Development
Discussions

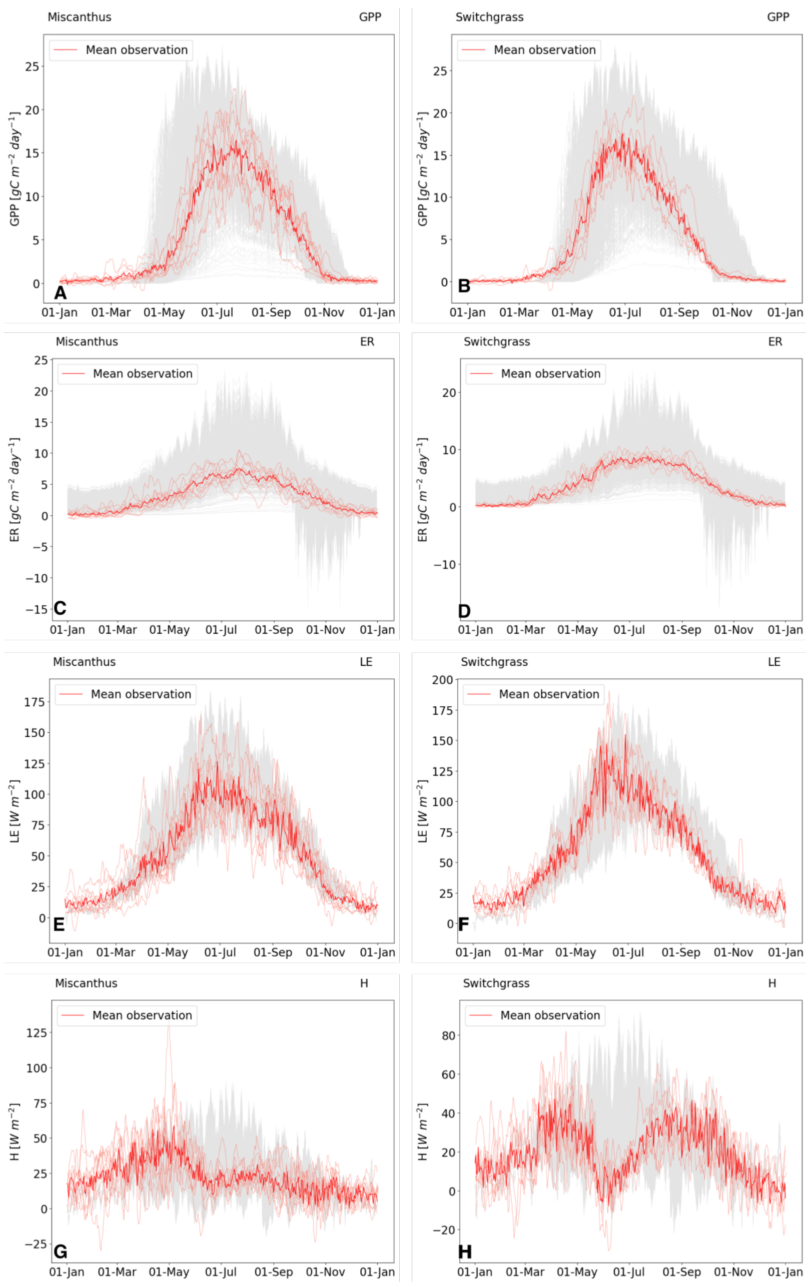

Figure 1. Simulated (grey lines) and observed (red lines) daily GPP ($gC\ m^{-2}\ day^{-1}$), ER ($gC\ m^{-2}\ day^{-1}$), LE ($W\ m^{-2}$) and, H ($W\ m^{-2}$) for miscanthus and switchgrass. Grey lines represent the simulated values for the 2000 ensemble members. Light red lines represent daily observed values from 2009-2018 while the thick red line is the daily average across the ten years. The observational data was collected at the University of Illinois Energy Farm from 2009-2018.

https://doi.org/10.5194/gmd-2021-244
Preprint. Discussion started: 21 July 2021

Geoscientific Model Development
Discussions

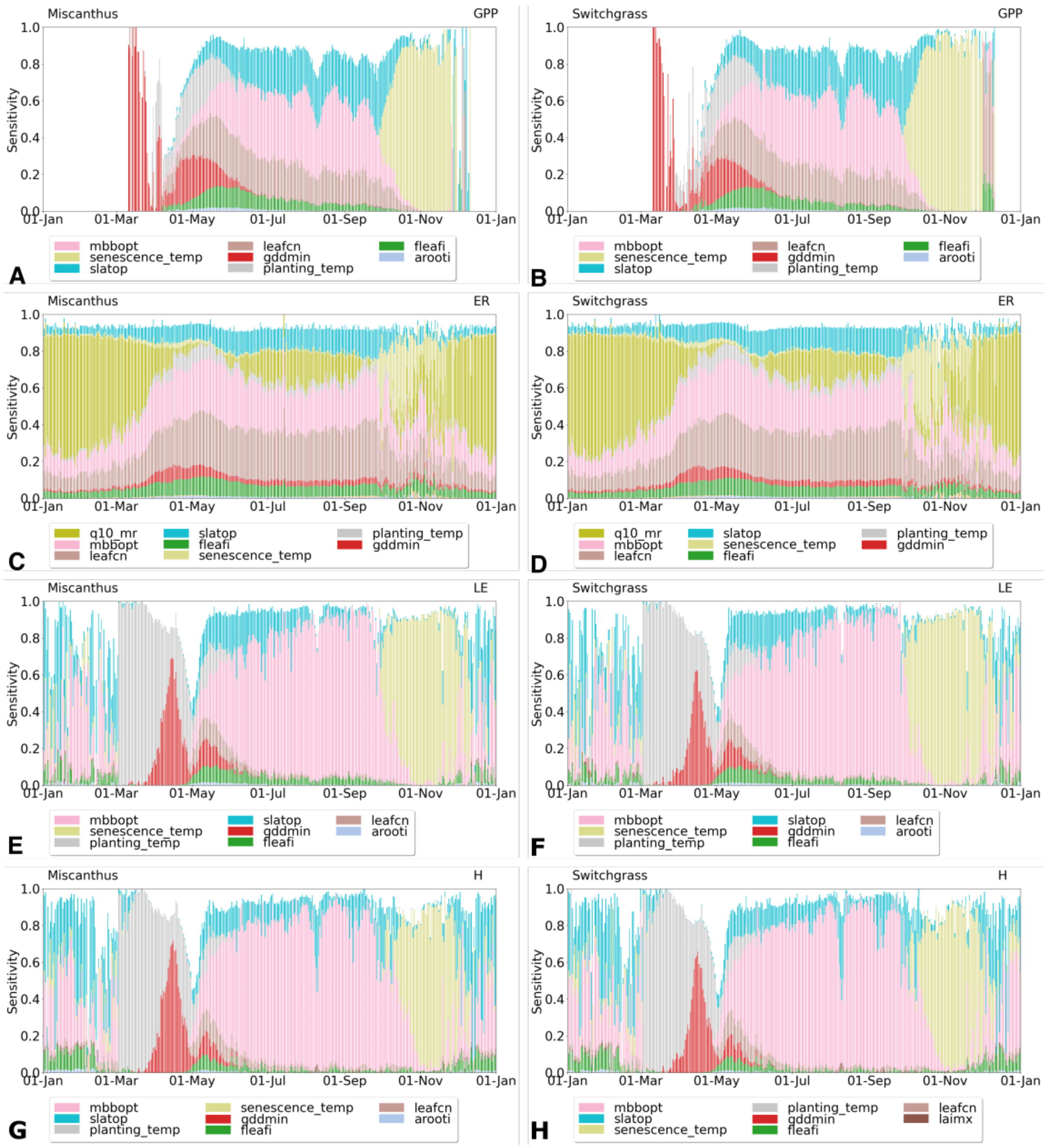

Figure 2. Main-effect Sobol sensitivity indices of the eighteen parameters for the daily GPP, ER, LE, and H outputs for miscanthus and switchgrass. The legend lists only the most influential parameters for the respective QoIs.

https://doi.org/10.5194/gmd-2021-244
Preprint. Discussion started: 21 July 2021

Geoscientific Model Development
Discussions

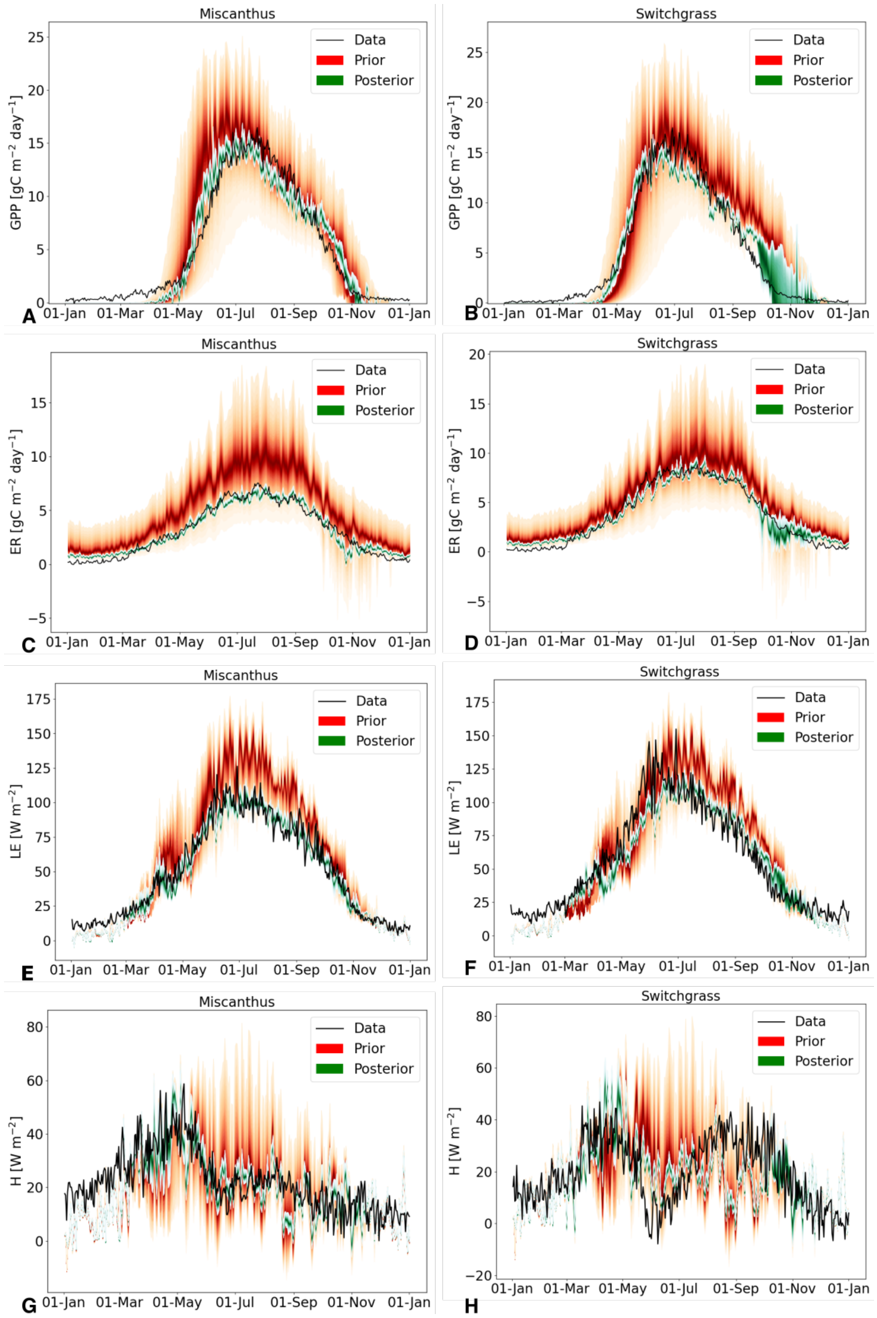

Figure 3. Observed vs. prior and posterior distribution of the modeled GPP ($gC\ m^{-2}\ day^{-1}$), ER ($gC\ m^{-2}\ day^{-1}$), LE ($W\ m^{-2}$) and, H ($W\ m^{-2}$) for miscanthus and switchgrass. The prior distribution (red shade) represents the daily simulated values for the 2000 ensemble members while the posterior distribution (green shade) represents the calibrated values estimated with the optimized parameters. A calibration window from 60 – 330 days and 60 – 270 days was utilized for miscanthus and switchgrass, respectively. The black line represents observed average daily values from 2009-2018 collected at the University of Illinois Energy Farm.

https://doi.org/10.5194/gmd-2021-244
Preprint. Discussion started: 21 July 2021

Geoscientific Model Development Discussions
Open Access

Table 2. Optimized parameter values for five most sensitive parameters based on maximum a posteriori (MAP) estimates

Parameter	ELM variable	Description	Input range	Miscanthus				Switchgrass			
				GPP	ER	LE	H	GPP	ER	LE	H
$\overline{T}_p$	planting_temp	Average 10-day temperature required for plant emergence	275 – 285	-	-	278	282	-	-	276	277
$\overline{GDD}^{min}$	gddmin	Minimum growing degree days	50 – 320	102	-	57	76	59	-	95	50
$\overline{T}_s$	senescence_temp	Average 10-day temperature for leaf senescence	280 – 290	285	-	285	284	290	289	281	283
$\overline{a}^i_{leaf}$	fleafi	Leaf CN allocation coefficient	0.5 – 0.95	-	0.74	-	-	-	-	-	-
	leafcn	Leaf CN ratio	15 – 35	35*	34	-	-	33	34	-	-
	slatop	Specific leaf area (SLA) at top of canopy	0.01 – 0.07	0.02	0.06	0.04	0.02	0.07*	0.07*	0.04	0.03
	q10_mr	Temperature sensitivity for MR	1.3 – 3.3	-	2.41	-	-	-	2.63	-	-
	mbbopt	Ball–Berry model equation slope	4 – 12	5.88	5.94	4.31*	7.3	8.8	11.8*	5	7.3

* - The pdf of the optimized parameter range was skewed to either side of the input range.

https://doi.org/10.5194/gmd-2021-244
Preprint. Discussion started: 21 July 2021

Table 3. RMSE, percent bias, correlation coefficient, and R^2 between observations and mean of surrogate based posterior simulations. All listed R^2 are significant with $p < 0.01$.

	Miscanthus within calibration window (60 – 330)				Switchgrass within calibration window (60 – 270)			
	GPP	ER	LE	H	GPP	ER	LE	H
RMSE	1.48	2.74	62.59	21.3	1.56	3.51	77.94	21.29
Percent bias	-0.2%	28.7%	-90.5%	-61.9%	-3.98%	32%	-89.9%	-52.1%
Corr. coeff.	0.96	0.95	0.94	-0.31	0.96	0.94	0.91	-0.5
R^2	0.92	0.90	0.88	0.10	0.92	0.88	0.83	0.25
	Miscanthus considering all 365 days				Switchgrass considering all 365 days			
RMSE	1.28	0.56	8.18	10.4	1.46	0.69	14.12	13.03
Percent bias	-1.73%	1.7%	-4.27%	-9.96%	-6.22%	3.16%	-8.27%	-1.97%
Corr. coeff.	0.97	0.97	0.97	0.65	0.97	0.98	0.94	0.45
R^2	0.94	0.94	0.94	0.42	0.94	0.96	0.88	0.20

Code and data availability. The code for ELMv1 is available on GitHub (https://github.com/E3SM-Project/E3SM). The UIUC Energy Farm data used in this study is in the process of joining the AmeriFlux network (Site ID - US-UiC). Data will be made available through the Ameriflux website soon).

Appendix A

A1

https://doi.org/10.5194/gmd-2021-244
Preprint. Discussion started: 21 July 2021

Geoscientific Model Development
Discussions

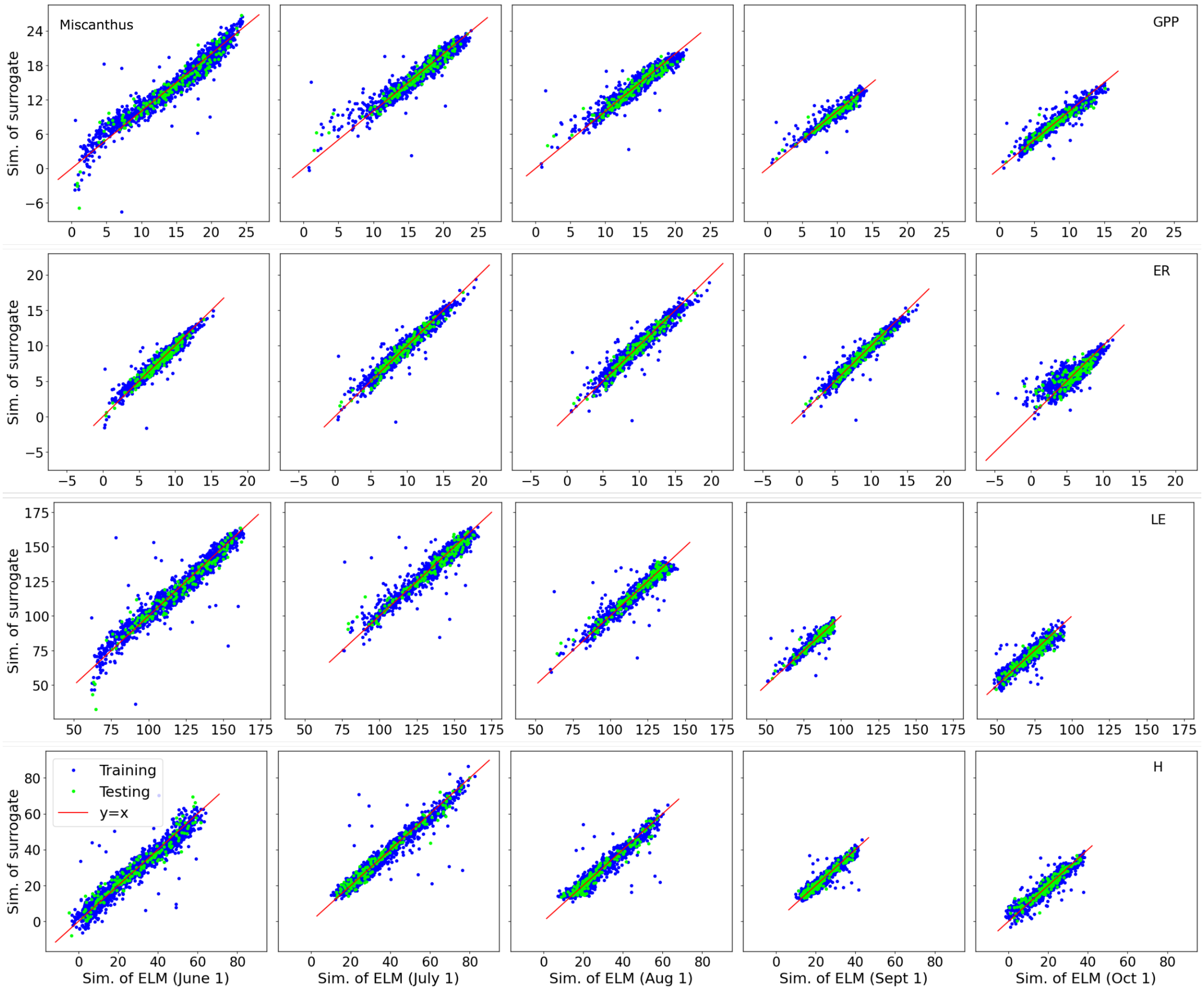

Figure A1. Scatter plot of ELM and surrogate model simulations for miscanthus for the four QoIs for the first day of June, July, August, September, and October.

https://doi.org/10.5194/gmd-2021-244
Preprint. Discussion started: 21 July 2021

Geoscientific Model Development
Discussions
Open Access

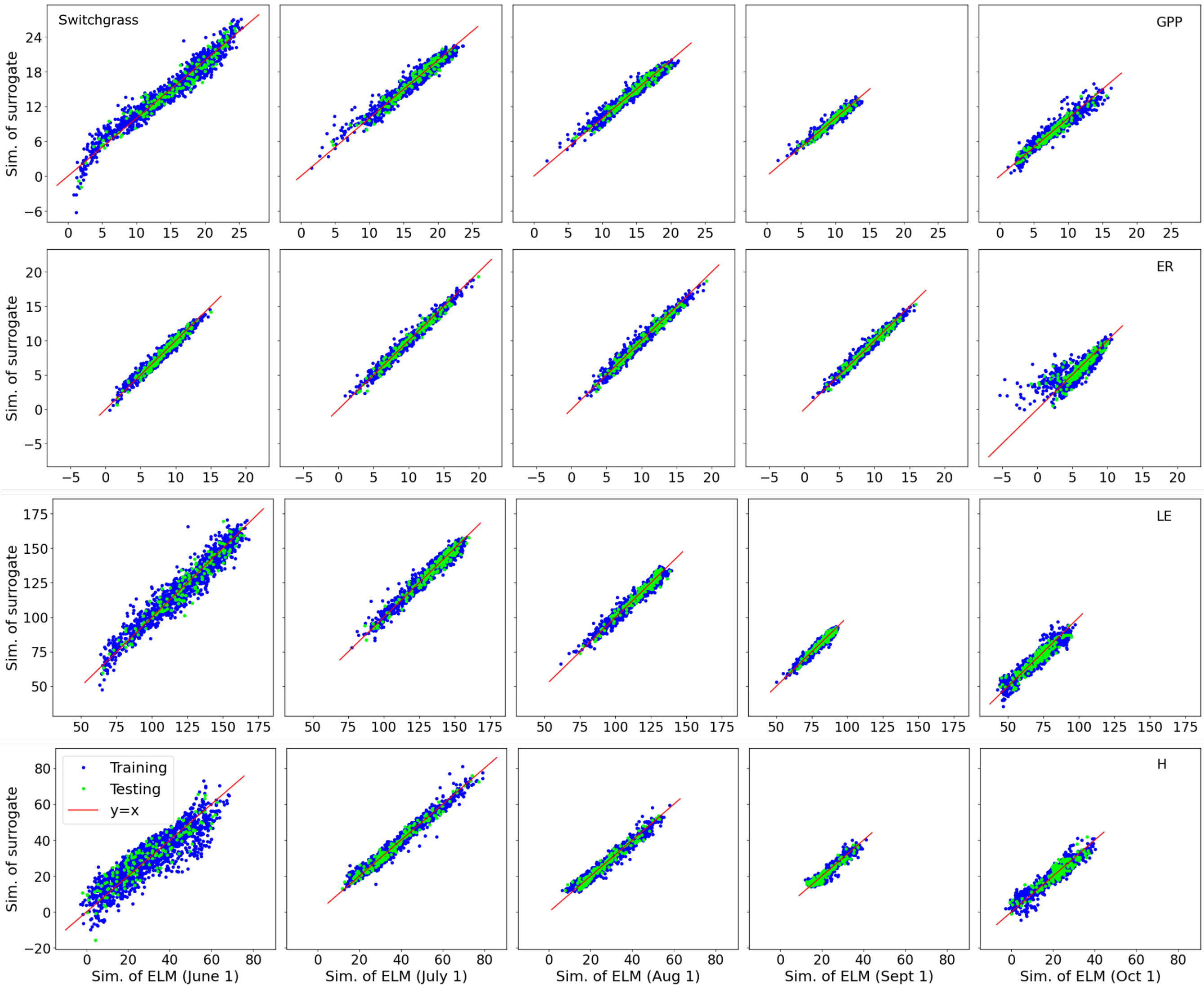

Figure A2. Same as Figure A1 but for switchgrass.

https://doi.org/10.5194/gmd-2021-244
Preprint. Discussion started: 21 July 2021

Geoscientific Model Development Discussions
Open Access
EGU

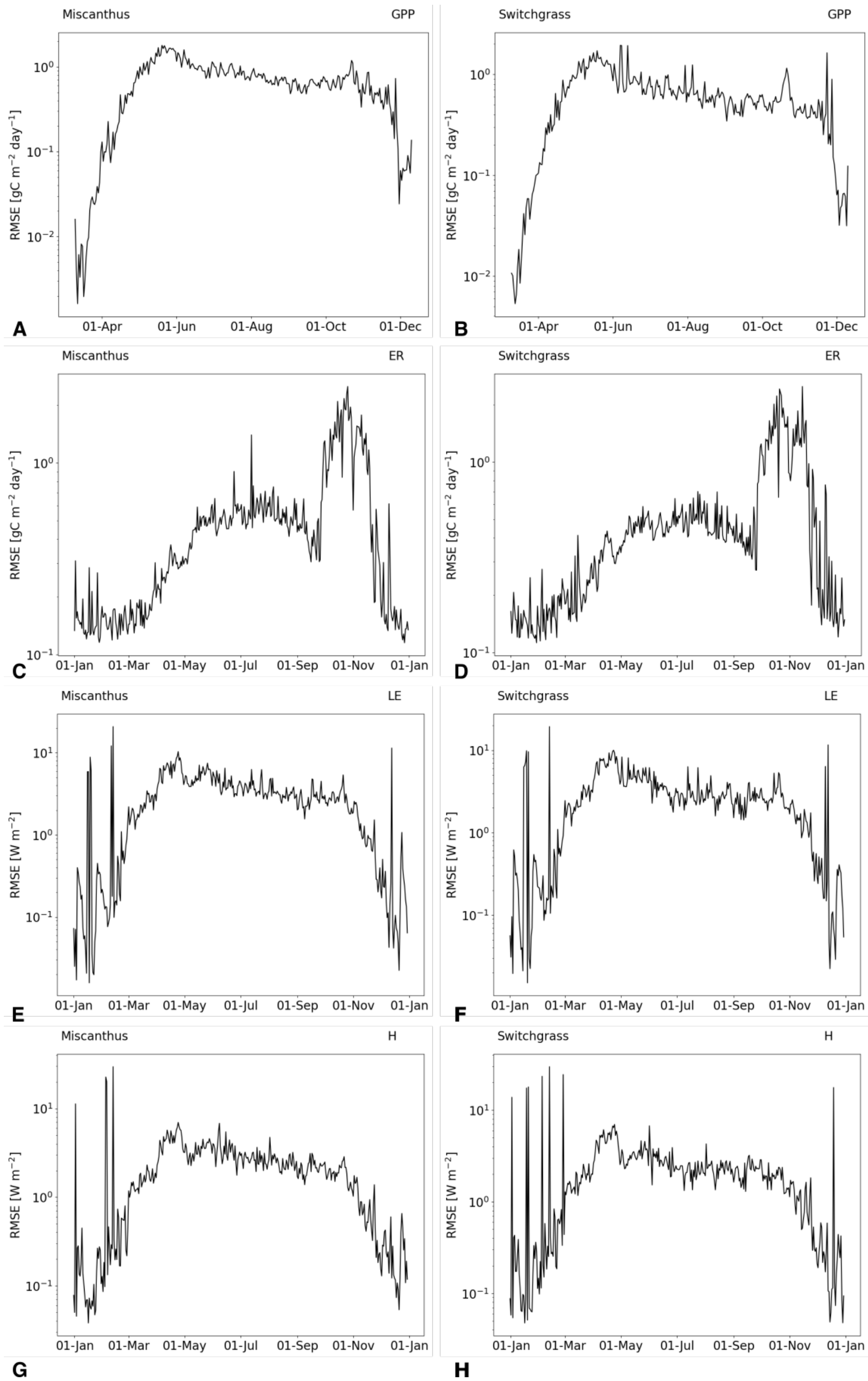

Figure A3. Root mean square error (RMSE) compared to the ELM simulations for the validation points (shown in green dots in Figure A1 and A2. The errors are shown for each day of the year for the four QoIs and both perennial bioenergy crops.

https://doi.org/10.5194/gmd-2021-244
Preprint. Discussion started: 21 July 2021

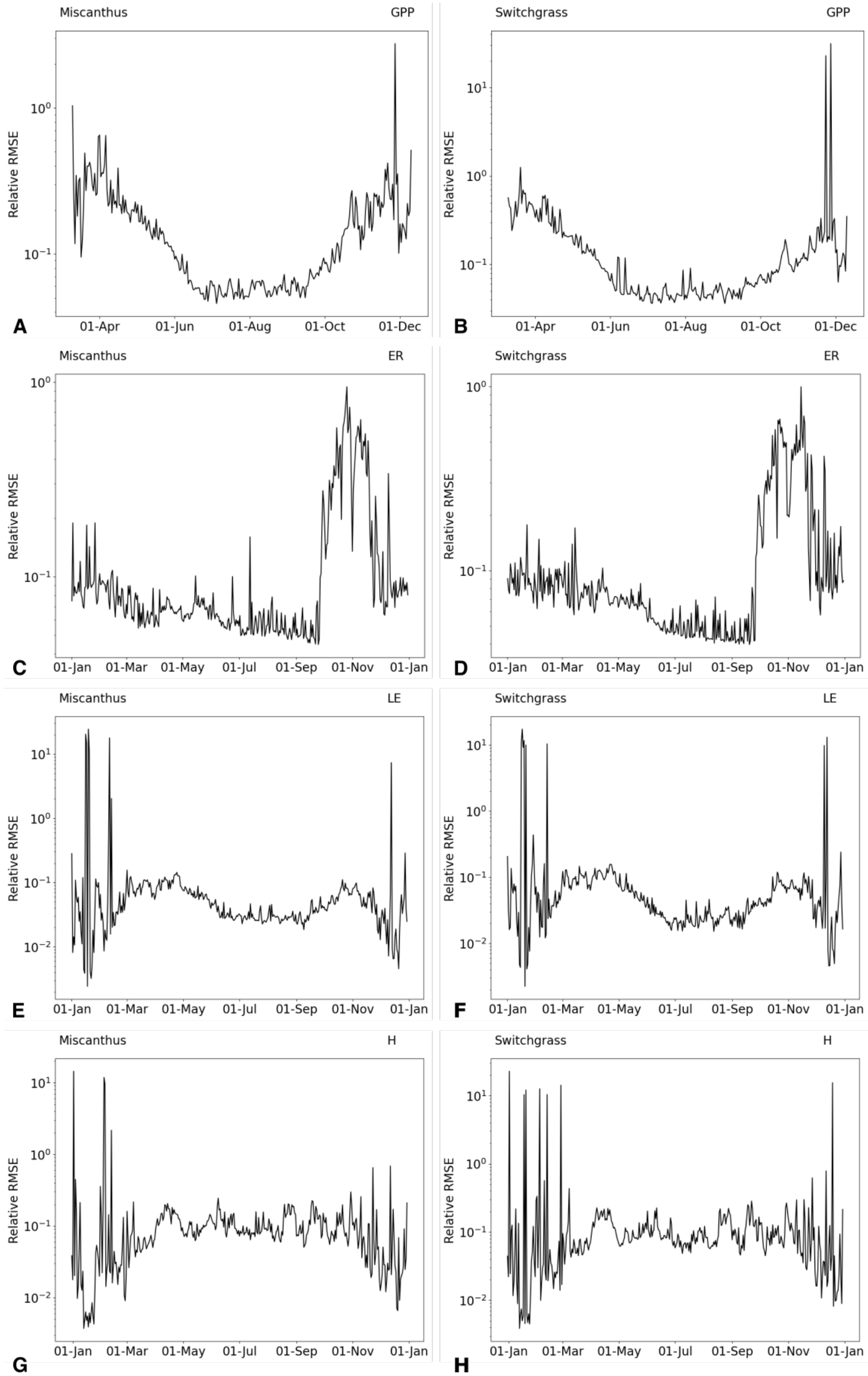

Figure A4. Same as Figure A3 but showing relative RMSE between surrogate and ELM simulations for each day of the year.

https://doi.org/10.5194/gmd-2021-244
Preprint. Discussion started: 21 July 2021

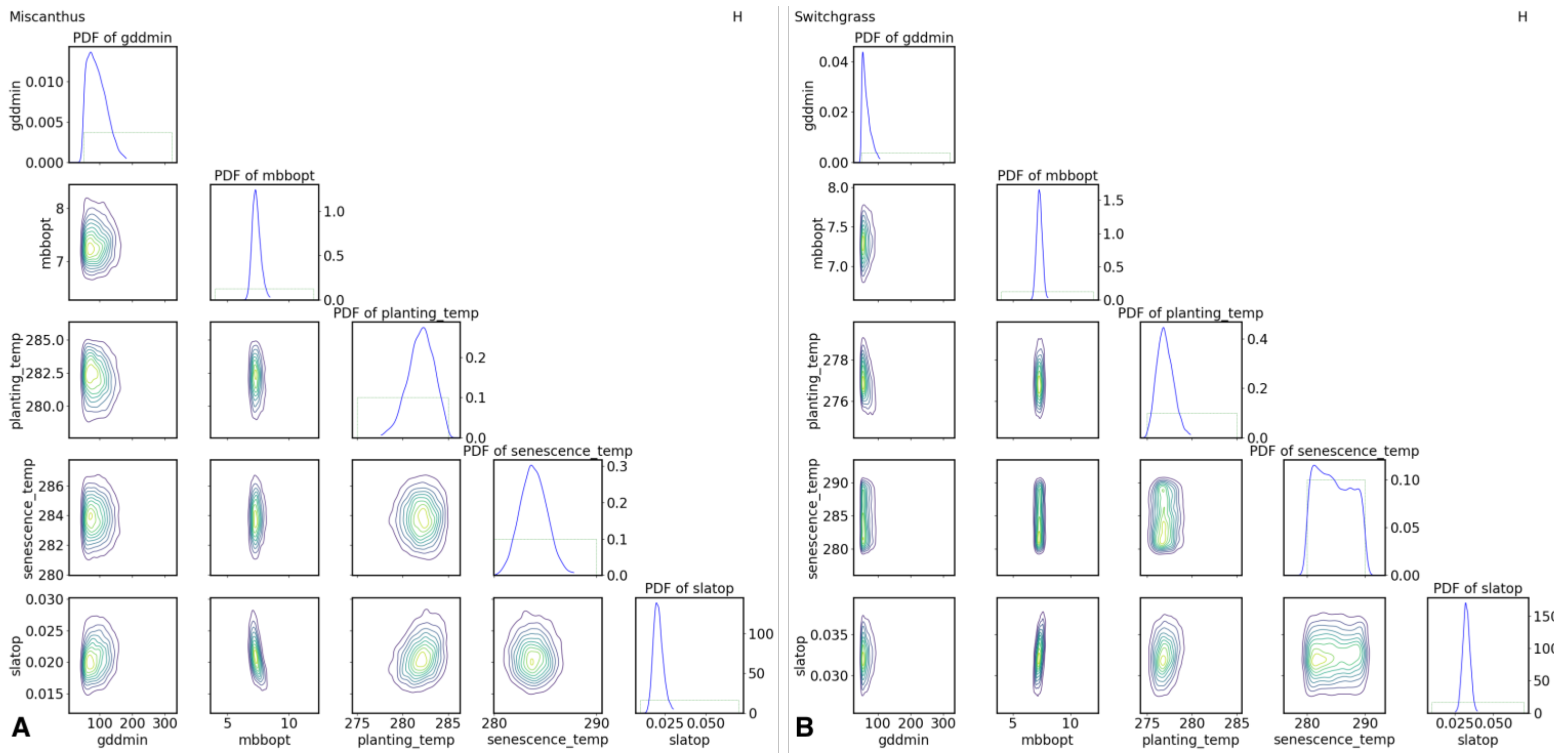

Figure A5. Posterior PDF of the five most sensitive parameters for GPP: `gddmin`, `leafcn`, `mbbopt`, `senescence_temp`, and `slattop` (Figure 2). The prior range for the parameters — `gddmin` (50 – 320); `leafcn` (15 – 35); `mbbopt` (4 – 12); `senescence_temp` (280 – 290) and; `slatop` (0.01 – 0.07) — is represented by the dotted green rectangles.

https://doi.org/10.5194/gmd-2021-244
Preprint. Discussion started: 21 July 2021

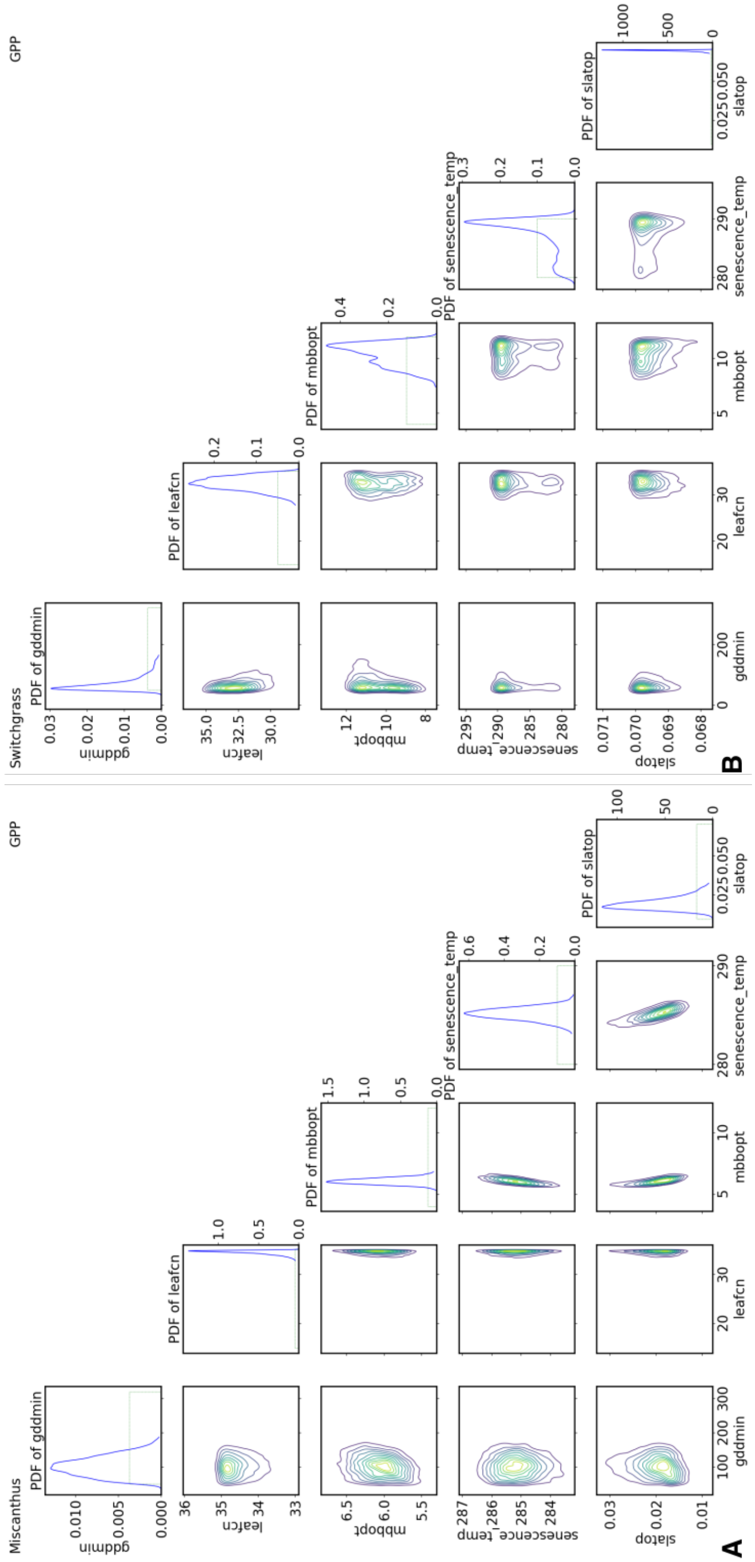

Figure A6. Same as Figure A5 but for ER.

https://doi.org/10.5194/gmd-2021-244
Preprint. Discussion started: 21 July 2021

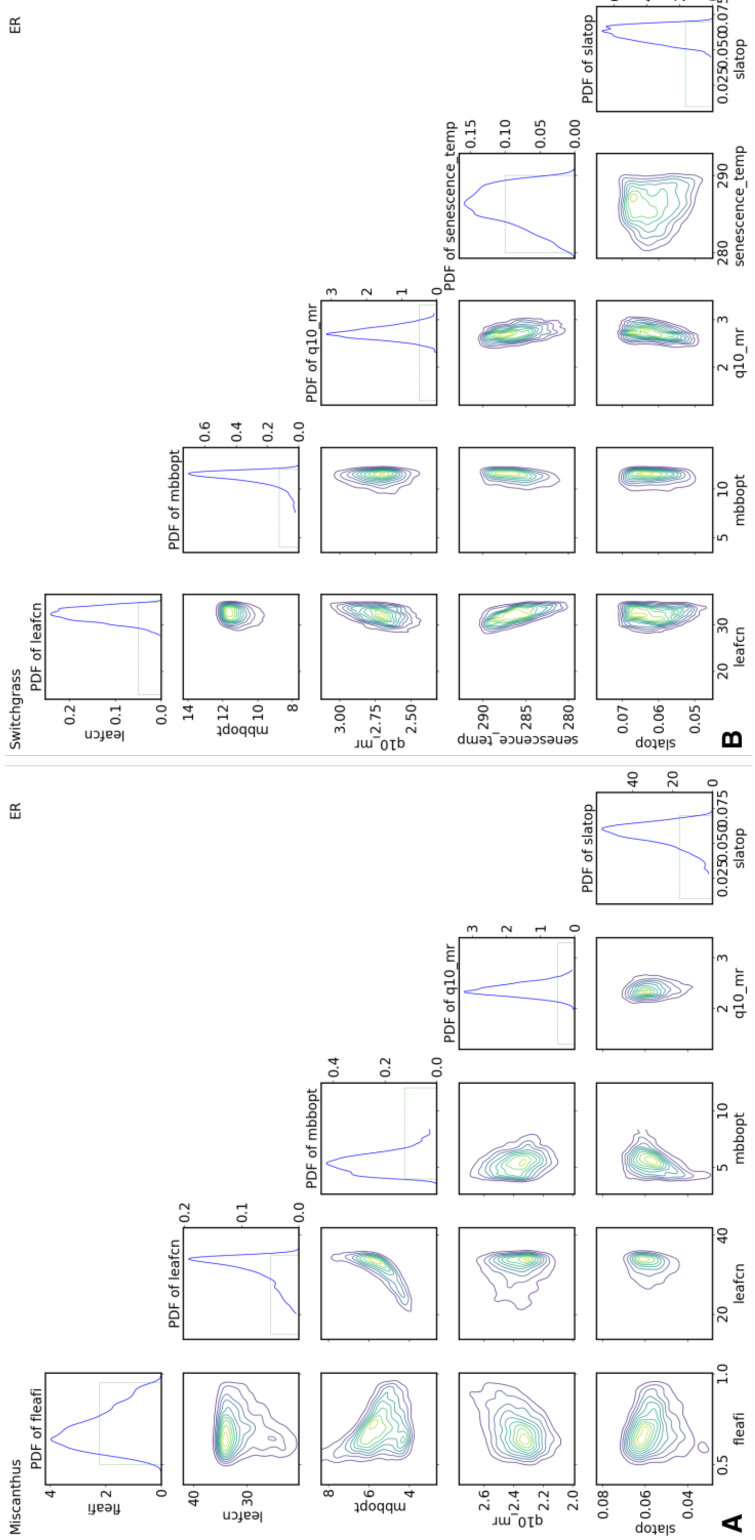

Figure A7. Same as Figure A5 but for LE.

https://doi.org/10.5194/gmd-2021-244
Preprint. Discussion started: 21 July 2021

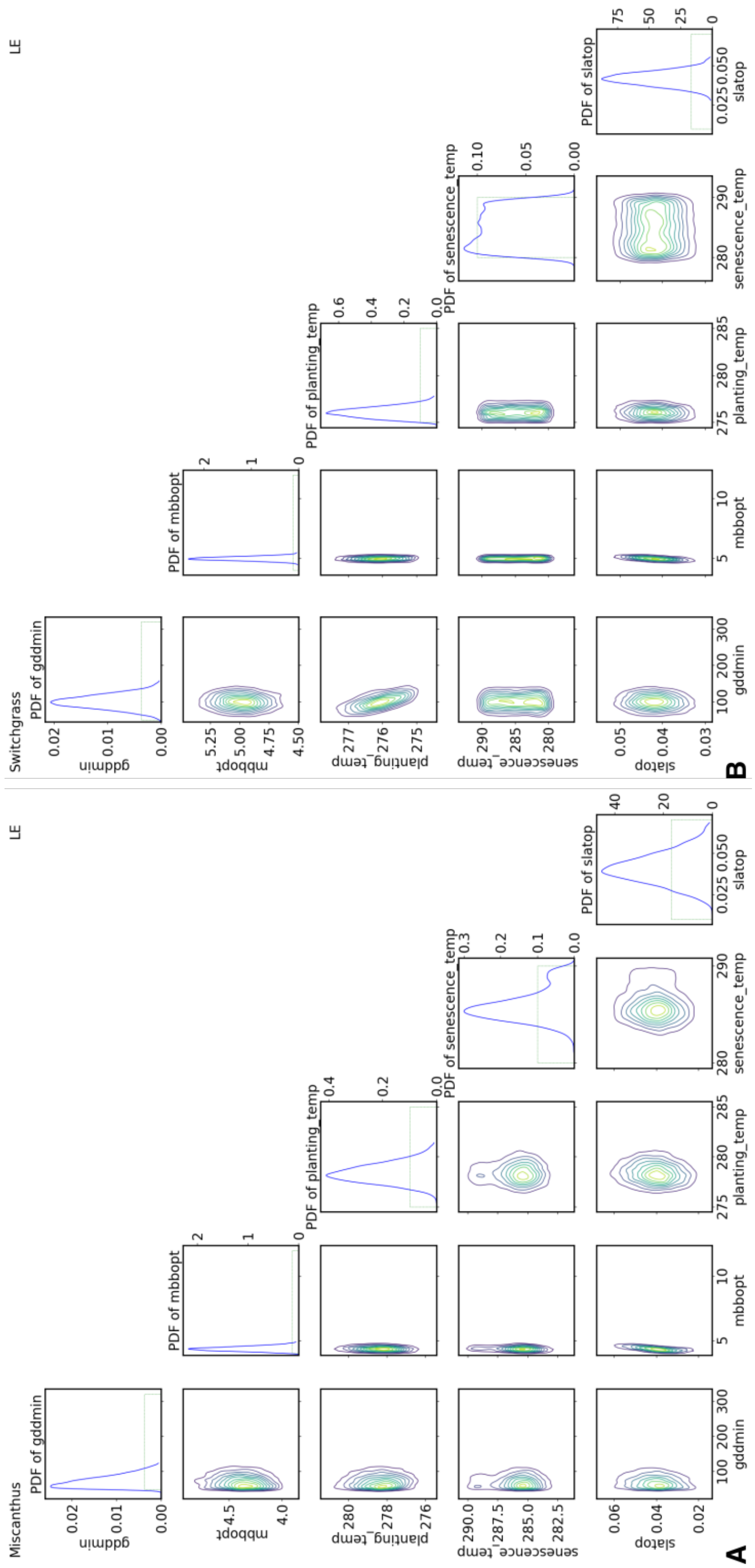

Figure A8. Same as Figure A5 but for H.

https://doi.org/10.5194/gmd-2021-244
Preprint. Discussion started: 21 July 2021

Table A1. Impact of calibration window on RMSE, percent bias, and optimized parameter distribution for miscanthus and switchgrass GPP.

	Miscanthus - GPP		Switchgrass - GPP	
Calibration window	RMSE	Percent bias	RMSE	Percent bias
0 – 365	1.22	-2.76%	1.48	-7.0%
60 – 270	1.42	-0.64%	1.56	-4.10%
60 – 300	1.67	-3.60%	1.7	-7.13%
60 – 330	1.51	-0.05%	1.7	-5.40%

Author contributions. TEXT

ES, KVC, BB-L, and BAD, designed the study. ES developed the model code, performed the simulations, and analyzed the results with contributions from KVC, BB-L, BAD, DMR and KS. All authors contributed to the writing of the manuscript.

Competing interests. The authors declare that there are no real or perceived financial conflicts of interest.

Acknowledgements. This research was supported as part of the Energy Exascale Earth System Model (E3SM) project, funded by the U.S. Department of Energy, Office of Science, Office of Biological and Environmental Research. The Pacific Northwest National Laboratory is operated by Battelle for the US Department of Energy under Contract DE-AC05-76RLO1830. Sandia National Laboratories is a multimission laboratory managed and operated by National Technology and Engineering Solutions of Sandia, LLC, a wholly owned subsidiary of Honeywell International Inc., for the U.S. Department of Energy's National Nuclear Security Administration under contract DE-NA0003525.

https://doi.org/10.5194/gmd-2021-244
Preprint. Discussion started: 21 July 2021

Geoscientific Model Development Discussions

References

Ali, A. A., Xu, C., Rogers, A., Fisher, R. A., Wullschleger, S. D., Massoud, E., Vrugt, J. A., Muss, J. D., McDowell, N. G., Fisher, J. B., et al.: A global scale mechanistic model of photosynthetic capacity (LUNA V1. 0), Geoscientific Model Development, 9, 587–606, 2016.

Anderson-Teixeira, K. J., Masters, M. D., Black, C. K., Zeri, M., Hussain, M. Z., Bernacchi, C. J., and DeLucia, E. H.: Altered belowground carbon cycling following land-use change to perennial bioenergy crops, Ecosystems, 16, 508–520, 2013.

Boas, T., Bogena, H., Grünwald, T., Heinesch, B., Ryu, D., Schmidt, M., Vereecken, H., Western, A., and Hendricks Franssen, H.-J.: Improving the representation of cropland sites in the Community Land Model (CLM) version 5.0, Geoscientific Model Development, 14, 573–601, 2021.

Burrows, S., Maltrud, M., Yang, X., Zhu, Q., Jeffery, N., Shi, X., Ricciuto, D., Wang, S., Bisht, G., Tang, J., et al.: The DOE E3SM v1. 1 biogeochemistry configuration: Description and simulated ecosystem-climate responses to historical changes in forcing, Journal of Advances in Modeling Earth Systems, 12, e2019MS001 766, 2020.

Cheng, Y., Huang, M., Chen, M., Guan, K., Bernacchi, C., Peng, B., and Tan, Z.: Parameterizing perennial bioenergy crops in Version 5 of the Community Land Model based on site-level observations in the Central Midwestern United States, Journal of Advances in Modeling Earth Systems, 12, 2020.

Cheng, Y., Huang, M., Zhu, B., Bisht, G., Zhou, T., Liu, Y., Song, F., and He, X.: Validation of the Community Land Model Version 5 Over the Contiguous United States (CONUS) Using In Situ and Remote Sensing Data Sets, Journal of Geophysical Research: Atmospheres, 126, e2020JD033 539, 2021.

Crestaux, T., Le Maître, O., and Martinez, J.: Polynomial Chaos Expansion for Sensitivity Analysis, Reliability Engineering & System Safety, 94, 1161–1172, 2009.

Debusschere, B., Sargsyan, K., Safta, C., and Chowdhary, K. S.: UQTk: A C++/Python Toolkit for Uncertainty Quantification., Tech. rep., Sandia National Lab.(SNL-CA), Livermore, CA (United States), 2016.

Dietzel, R., Liebman, M., and Archontoulis, S.: A deeper look at the relationship between root carbon pools and the vertical distribution of the soil carbon pool, Soil, 3, 139–152, 2017.

Dohleman, F., Heaton, E., Leakey, A., and Long, S.: Does greater leaf-level photosynthesis explain the larger solar energy conversion efficiency of Miscanthus relative to switchgrass?, Plant, cell & environment, 32, 1525–1537, 2009.

Drewniak, B.: Simulating dynamic roots in the energy exascale earth system land model, Journal of Advances in Modeling Earth Systems, 11, 338–359, 2019.

Drewniak, B., Song, J., Prell, J., Kotamarthi, V., and Jacob, R.: Modeling agriculture in the community land model, Geoscientific Model Development, 6, 495–515, 2013.

Duarte, H. F., Raczka, B. M., Ricciuto, D. M., Lin, J. C., Koven, C. D., Thornton, P. E., Bowling, D. R., Lai, C.-T., Bible, K. J., and Ehleringer, J. R.: Evaluating the Community Land Model (CLM4. 5) at a coniferous forest site in northwestern United States using flux and carbon-isotope measurements, Biogeosciences, 14, 4315–4340, 2017.

FAO: FAOSTAT. Food and Agriculture Organization of the United Nations, Tech. rep., FAO, 2021.

Fargione, J., Hill, J., Tilman, D., Polasky, S., and Hawthorne, P.: Land clearing and the biofuel carbon debt, Science, 319, 1235–1238, 2008.

Georgescu, M., Lobell, D. B., and Field, C. B.: Direct climate effects of perennial bioenergy crops in the United States, Proceedings of the National Academy of Sciences, 108, 4307–4312, 2011.

Ghanem, R. and Spanos, P.: Stochastic Finite Elements: A Spectral Approach, Springer Verlag, New York, 1991.

IPCC: Global warming of 1.5° C: an IPCC special report on the impacts of global warming of 1.5° C above pre-industrial levels and related global greenhouse gas emission pathways, in the context of strengthening the global response to the threat of climate change, sustainable development, and efforts to eradicate poverty, Intergovernmental Panel on Climate Change, 2018.

Jiao, X., Kørup, K., Andersen, M. N., Petersen, K. K., Prade, T., Jeżowski, S., Ornatowski, S., Górynowicz, B., Spitz, I., Lærke, P. E., et al.: Low-temperature leaf photosynthesis of a Miscanthus germplasm collection correlates positively to shoot growth rate and specific leaf area, Annals of botany, 117, 1229–1239, 2016.

Klein Goldewijk, K., Beusen, A., Doelman, J., and Stehfest, E.: Anthropogenic land use estimates for the Holocene–HYDE 3.2, Earth System Science Data, 9, 927–953, 2017.

Lambert, F. H., Harris, G. R., Collins, M., Murphy, J. M., Sexton, D. M., and Booth, B. B.: Interactions between perturbations to different Earth system components simulated by a fully-coupled climate model, Climate dynamics, 41, 3055–3072, 2013.

Langholtz, M. H., Stokes, B. J., and Eaton, L. M.: 2016 Billion-ton report: Advancing domestic resources for a thriving bioeconomy, Volume 1: Economic availability of feedstock, Oak Ridge National Laboratory, Oak Ridge, Tennessee, managed by UT-Battelle, LLC for the US Department of Energy, 2016, 1–411, 2016.

Lee, D., Doolittle, J., and Owens, V.: Soil carbon dioxide fluxes in established switchgrass land managed for biomass production, Soil Biology and Biochemistry, 39, 178–186, 2007.

Levis, S.: Modeling vegetation and land use in models of the Earth System, Wiley Interdisciplinary Reviews: Climate Change, 1, 840–856, 2010.

Levis, S., Bonan, G. B., Kluzek, E., Thornton, P. E., Jones, A., Sacks, W. J., and Kucharik, C. J.: Interactive crop management in the Community Earth System Model (CESM1): Seasonal influences on land–atmosphere fluxes, Journal of Climate, 25, 4839–4859, 2012.

Li, W., Yue, C., Ciais, P., Chang, J., Goll, D., Zhu, D., Peng, S., and Jornet-Puig, A.: ORCHIDEE-MICT-BIOENERGY: an attempt to represent the production of lignocellulosic crops for bioenergy in a global vegetation model, Geoscientific Model Development, 11, 2249–2272, 2018.

Littleton, E. W., Harper, A. B., Vaughan, N. E., Oliver, R. J., Duran-Rojas, M. C., and Lenton, T. M.: JULES-BE: representation of bioenergy crops and harvesting in the Joint UK Land Environment Simulator vn5. 1, Geoscientific Model Development, 13, 1123–1136, 2020.

Liu, X., Chen, F., Barlage, M., Zhou, G., and Niyogi, D.: Noah-MP-Crop: Introducing dynamic crop growth in the Noah-MP land surface model, Journal of Geophysical Research: Atmospheres, 121, 13–953, 2016.

Lokupitiya, E., Denning, S., Paustian, K., Baker, I., Schaefer, K., Verma, S., Meyers, T., Bernacchi, C., Suyker, A., and Fischer, M.: Incorporation of crop phenology in Simple Biosphere Model (SiBcrop) to improve land-atmosphere carbon exchanges from croplands, Biogeosciences, 6, 969–986, 2009.

Lombardozzi, D., Bonan, G., Wieder, W., Grandy, A., Morris, C., and Lawrence, D.: Cover crops may cause winter warming in snow-covered regions, Geophysical Research Letters, 45, 9889–9897, 2018.

Lombardozzi, D. L., Lu, Y., Lawrence, P. J., Lawrence, D. M., Swenson, S., Oleson, K. W., Wieder, W. R., and Ainsworth, E. A.: Simulating agriculture in the Community Land Model version 5, Journal of Geophysical Research: Biogeosciences, 125, e2019JG005 529, 2020.

Lu, D. and Ricciuto, D.: Efficient surrogate modeling methods for large-scale Earth system models based on machine-learning techniques, Geoscientific Model Development, 12, 1791–1807, 2019.

Lu, D., Ricciuto, D., Stoyanov, M., and Gu, L.: Calibration of the E3SM land model using surrogate-based global optimization, Journal of Advances in Modeling Earth Systems, 10, 1337–1356, 2018.

Ma, B. and Dwyer, L.: Maize kernel moisture, carbon and nitrogen concentrations from silking to physiological maturity, Canadian Journal of Plant Science, 81, 225–232, 2001.

McDermid, S., Mearns, L., and Ruane, A.: Representing agriculture in E arth S ystem M odels: Approaches and priorities for development, Journal of Advances in Modeling Earth Systems, 9, 2230–2265, 2017.

Moore, C. E., Berardi, D. M., Blanc-Betes, E., Dracup, E. C., Egenriether, S., Gomez-Casanovas, N., Hartman, M. D., Hudiburg, T., Kantola, I., Masters, M. D., et al.: The carbon and nitrogen cycle impacts of reverting perennial bioenergy switchgrass to an annual maize crop rotation, GCB Bioenergy, 12, 941–954, 2020.

Moore, C. E., von Haden, A. C., Burnham, M. B., Kantola, I. B., Gibson, C. D., Blakely, B. J., Dracup, E. C., Masters, M. D., Yang, W. H., DeLucia, E. H., et al.: Ecosystem-scale biogeochemical fluxes from three bioenergy crop candidates: How energy sorghum compares to maize and miscanthus, GCB Bioenergy, 13, 445–458, 2021.

Mueller, N. D., Butler, E. E., McKinnon, K. A., Rhines, A., Tingley, M., Holbrook, N. M., and Huybers, P.: Cooling of US Midwest summer temperature extremes from cropland intensification, Nature Climate Change, 6, 317–322, 2016.

Oleson, K., Lawrence, D., Bonan, G., Drewniak, B., Huang, M., Koven, C., Levis, S., Li, F., Riley, W., Subin, Z., et al.: Technical description of version 4.5 of the Community Land Model (CLM), NCAR Technical Note: NCAR/TN-503+ STR, National Center for Atmospheric Research (NCAR), Boulder, CO, USA, https://doi. org/10.5065/D6RR1W7M, 2013.

Osborne, T., Gornall, J., Hooker, J., Williams, K., Wiltshire, A., Betts, R., and Wheeler, T.: JULES-crop: a parametrisation of crops in the Joint UK Land Environment Simulator, Geoscientific Model Development, 8, 1139–1155, 2015.

Popp, A., Calvin, K., Fujimori, S., Havlik, P., Humpenöder, F., Stehfest, E., Bodirsky, B. L., Dietrich, J. P., Doelmann, J. C., Gusti, M., et al.: Land-use futures in the shared socio-economic pathways, Global Environmental Change, 42, 331–345, 2017.

Qian, Y., Wan, H., Yang, B., Golaz, J.-C., Harrop, B., Hou, Z., Larson, V. E., Leung, L. R., Lin, G., Lin, W., et al.: Parametric sensitivity and uncertainty quantification in the version 1 of E3SM atmosphere model based on short perturbed parameter ensemble simulations, Journal of Geophysical Research: Atmospheres, 123, 13–046, 2018.

Ricciuto, D., Sargsyan, K., and Thornton, P.: The impact of parametric uncertainties on biogeochemistry in the E3SM land model, Journal of Advances in Modeling Earth Systems, 10, 297–319, 2018.

Robertson, A. D., Whitaker, J., Morrison, R., Davies, C. A., Smith, P., and McNamara, N. P.: A Miscanthus plantation can be carbon neutral without increasing soil carbon stocks, GCB Bioenergy, 9, 645–661, 2017.

Saltelli, A., Annoni, P., Azzini, I., Campolongo, F., Ratto, M., and Tarantola, S.: Variance based sensitivity analysis of model output. Design and estimator for the total sensitivity index, Computer physics communications, 181, 259–270, 2010.

Sargsyan, K.: Surrogate Models for Uncertainty Propagation and Sensitivity Analysis, in: Handbook of Uncertainty Quantification, edited by Ghanem, R., Higdon, D., and Owhadi, H., Springer, 2017.

Sargsyan, K., Safta, C., Najm, H., Debusschere, B., Ricciuto, D., and Thornton, P.: Dimensionality reduction for complex models via Bayesian compressive sensing, International Journal of Uncertainty Quantification, 4, 63–93, https://doi.org/10.1615/Int.J.UncertaintyQuantification.2013006821, 2014.

Searchinger, T., Heimlich, R., Houghton, R. A., Dong, F., Elobeid, A., Fabiosa, J., Tokgoz, S., Hayes, D., and Yu, T.-H.: Use of US croplands for biofuels increases greenhouse gases through emissions from land-use change, Science, 319, 1238–1240, 2008.

Seguin, B., Arrouays, D., Balesdent, J., Soussana, J.-F., Bondeau, A., Smith, P., Zaehle, S., De Noblet, N., and Viovy, N.: Moderating the impact of agriculture on climate, Agricultural and Forest meteorology, 142, 278–287, 2007.

https://doi.org/10.5194/gmd-2021-244
Preprint. Discussion started: 21 July 2021

Geoscientific Model Development
Discussions

Shi, M., Fisher, J. B., Brzostek, E. R., and Phillips, R. P.: Carbon cost of plant nitrogen acquisition: global carbon cycle impact from an improved plant nitrogen cycle in the Community Land Model, Global change biology, 22, 1299–1314, 2016.

Skinner, R. H. and Adler, P. R.: Carbon dioxide and water fluxes from switchgrass managed for bioenergy production, Agriculture, ecosystems & environment, 138, 257–264, 2010.

Smith, C. M., David, M. B., Mitchell, C. A., Masters, M. D., Anderson-Teixeira, K. J., Bernacchi, C. J., and DeLucia, E. H.: Reduced nitrogen losses after conversion of row crop agriculture to perennial biofuel crops, Journal of environmental quality, 42, 219–228, 2013.

Sobol, I. M.: Global sensitivity indices for nonlinear mathematical models and their Monte Carlo estimates, Mathematics and computers in simulation, 55, 271–280, 2001.

Song, Y., Jain, A., and McIsaac, G.: Implementation of dynamic crop growth processes into a land surface model: evaluation of energy, water and carbon fluxes under corn and soybean rotation, Biogeosciences, 10, 8039–8066, 2013.

Song, Y., Jain, A. K., Landuyt, W., Kheshgi, H. S., and Khanna, M.: Estimates of biomass yield for perennial bioenergy grasses in the USA, BioEnergy Research, 8, 688–715, 2015.

Tarantola, A.: Inverse Problem Theory and Methods for Model Parameter Estimation, SIAM, 2005.

Tian, S., Cacho, J. F., Youssef, M. A., Chescheir, G. M., and Nettles, J. E.: Switchgrass growth and morphological changes under established pine-grass agroforestry systems in the lower coastal plain of North Carolina, United States, Biomass and Bioenergy, 83, 233–244, 2015.

Trócsányi, Z. K., Fieldsend, A., and Wolf, D.: Yield and canopy characteristics of switchgrass (Panicum virgatum L.) as influenced by cutting management, Biomass and Bioenergy, 33, 442–448, 2009.

Verge, X., De Kimpe, C., and Desjardins, R.: Agricultural production, greenhouse gas emissions and mitigation potential, Agricultural and forest meteorology, 142, 255–269, 2007.

Wu, X., Vuichard, N., Ciais, P., Viovy, N., Noblet-Ducoudré, N. d., Wang, X., Magliulo, V., Wattenbach, M., Vitale, L., Tommasi, P. D., et al.: ORCHIDEE-CROP (v0), a new process-based agro-land surface model: model description and evaluation over Europe, Geoscientific Model Development, 9, 857–873, 2016.

Yazaki, Y., Mariko, S., and Koizumi, H.: Carbon dynamics and budget in a Miscanthus sinensis grassland in Japan, Ecological Research, 19, 511–520, 2004.

Zeri, M., Anderson-Teixeira, K., Hickman, G., Masters, M., DeLucia, E., and Bernacchi, C. J.: Carbon exchange by establishing biofuel crops in Central Illinois, Agriculture, Ecosystems & Environment, 144, 319–329, 2011.

Zhu, P., Zhuang, Q., Eva, J., and Bernacchi, C.: Importance of biophysical effects on climate warming mitigation potential of biofuel crops over the conterminous United States, Gcb Bioenergy, 9, 577–590, 2017.